

# Flexible wire-like all-carbon supercapacitors based on porous core–shell carbon fibers†

Cite this: *J. Mater. Chem. A*, 2014, 2, 7250

Weijia Zhou,<sup>\*a</sup> Kai Zhou,<sup>a</sup> Xiaojun Liu,<sup>a</sup> Renzong Hu,<sup>b</sup> Hong Liu<sup>c</sup> and Shaowei Chen<sup>\*ad</sup>

Hierarchical porous carbon-based supercapacitors have been attracting intense attention due to their high and stable electrical double-layer capacitance that may be used for advanced technologies. In this study, porous core–shell carbon fibers were produced by a simple and fast acid oxidation treatment of carbon fibers, and the morphological and structural evolution were examined by SEM, TEM and Raman spectroscopic measurements. Detailed electrochemical characterizations showed that the resulting porous core–shell carbon fibers exhibited an excellent performance for charge storage with a specific capacitance of 98 F g<sup>-1</sup> at 0.5 A g<sup>-1</sup> in a 1 M H<sub>2</sub>SO<sub>4</sub> liquid electrolyte and 20.4 F g<sup>-1</sup> at 1 A g<sup>-1</sup> in a H<sub>2</sub>SO<sub>4</sub>/PVA solid electrolyte, and excellent capacitance retention at ~98.5% for the former and ~96% for the latter over 3000 cycles. The results demonstrated that porous core–shell carbon fibers might be used as effective electrode materials for the fabrication of wire-like all-carbon flexible supercapacitors with high physical flexibility and desirable electrochemical properties.

Received 18th December 2013  
Accepted 3rd March 2014

DOI: 10.1039/c3ta15280d

www.rsc.org/MaterialsA

## Introduction

Supercapacitors have been attracting extensive attention as a promising candidate for effective energy storage due to their high power performance, long life cycle, and safe operation that may be used for a wide range of applications.<sup>1</sup> As the charges are stored in the electrical double layer formed at the electrolyte–electrode interface, supercapacitors are generally composed of electrode materials with a high surface area, such as activated carbon,<sup>2</sup> graphene nanosheets,<sup>3</sup> ordered mesoporous carbons,<sup>4</sup> and carbon nanotubes.<sup>5</sup> In these carbon materials, the highly porous structures act as a bulk buffering reservoir for electrolytes so as to minimize the impedance of ion transport to the interior surfaces of the pores.

To harness these properties for practical applications, both large-scale synthesis and integration of advanced multifunctional carbon structures are required. Whereas three-dimensional graphene<sup>6</sup> and graphene aerogels<sup>7,8</sup> have been grown by chemical vapor deposition (CVD), large-quantity synthesis of

carbon nanostructures has remained a great challenge.<sup>9</sup> In addition, to fabricate flexible high-performance supercapacitors, one must also take into account the physical flexibility, electrochemical properties, and mechanical strength of the electrode materials.<sup>10</sup> Towards this end, carbon fibers have emerged as promising candidates as flexible substrates, because of their high mechanical flexibility and electrical conductivity. In fact, carbon fibers, which are mostly made of graphite flakes, have been used extensively as conductive substrates to construct a variety of composite structures, such as Zn<sub>2</sub>SnO<sub>4</sub>/MnO<sub>2</sub> core/shell carbon microfibers, WO<sub>3-x</sub>@Au@MnO<sub>2</sub> core–shell nanowires on carbon fabrics and cobalt oxide nanonet/carbon fiber paper.<sup>11</sup> Meanwhile, attempts have also been made to fabricate wire-shaped supercapacitors based on, for instance, elastic fiber@carbon nanotube sheets,<sup>12</sup> carbon fibers@pen ink,<sup>13</sup> and cotton thread@MnO<sub>2</sub>–carbon nanotube composites.<sup>14</sup> However, the use of carbon fibers for high-performance all-carbon electrical double-layer capacitors has been scarce.<sup>15,16</sup> Of these, Le *et al.* reported the preparation of a coaxial fiber supercapacitor, which consisted of carbon microfiber bundles coated with multiwalled carbon nanotubes as a core electrode and carbon nanofiber paper as an outer electrode, and exhibited a high capacitance of 6.3 mF cm<sup>-1</sup> (86.8 mF cm<sup>-2</sup>) with an excellent cycling performance and an energy density of 0.7 μW h cm<sup>-1</sup> (9.8 μW h cm<sup>-2</sup>) at a power density of 13.7 μW cm<sup>-1</sup> (189.4 μW cm<sup>-2</sup>).<sup>16</sup> However, the fabrication process of the device was rather complex.

Herein we report a simple process for the preparation of porous core–shell carbon fibers by a facile acid oxidation treatment. With excellent electrical conductivity and mechanical flexibility the porous carbon fibers were used for the

<sup>a</sup>New Energy Research Institute, School of Environment and Energy, South China University of Technology, Guangzhou Higher Education Mega Center, Guangzhou 510006, China. E-mail: eszhouwj@scut.edu.cn; Shaowei@ucsc.edu

<sup>b</sup>School of Materials Science and Engineering, South China University of Technology, Guangzhou Higher Education Mega Center, Guangzhou 510006, China

<sup>c</sup>State Key Laboratory of Crystal Materials, Center of Bio & Micro/Nano Functional Materials, Shandong University, 27 South Shanda Road, Jinan 250100, China

<sup>d</sup>Department of Chemistry and Biochemistry, University of California, 1156 High Street, Santa Cruz, California 95064, USA

† Electronic supplementary information (ESI) available: Calculations of specific capacitance, size histogram of carbon nanoparticles in the porous shells, specific surface area and pore size distribution, FTIR spectra, electrochemical impedance data, and additional CV data. See DOI: 10.1039/c3ta15280d

fabrication of wire-like all-carbon supercapacitors. The morphology and microstructure of the as-prepared core-shell carbon fibers were examined by means of scanning electron microscopy (SEM), transmission electron microscopy (TEM), infrared and Raman spectroscopy. Detailed electrochemical characterizations showed that the porous core-shell carbon fibers exhibited a high specific capacitance and excellent cyclability both in a liquid electrolyte (1 M H<sub>2</sub>SO<sub>4</sub>) and a solid electrolyte (H<sub>2</sub>SO<sub>4</sub>/PVA). The results demonstrated that core-shell carbon fibers might be promising candidates for the preparation of low-cost flexible wire-like all-carbon supercapacitors.

## Experimental

### Materials

All reagents were of analytical grade and used without further purification. Sulfuric acid (H<sub>2</sub>SO<sub>4</sub>), nitric acid (HNO<sub>3</sub>), and polyvinyl alcohol (PVA) (molecular weight 75 000–80 000) were purchased from Tianjin Chemical Reagents Co. Ltd in China. Carbon fibers were obtained from Fiber Glast Development Corporation in the USA. Water was supplied with a Barnstead Nanopure Water System (18.3 MΩ cm).

### Synthesis of porous core-shell carbon fibers

Porous core-shell carbon fibers were prepared by adopting a procedure in the literature.<sup>17</sup> In brief, 10 cm of carbon fibers (about 60 mg) was immersed into a mixture of concentrated H<sub>2</sub>SO<sub>4</sub> (30 mL) and HNO<sub>3</sub> (10 mL). The solution was sonicated for 2 h and heated for 10 min at 120 °C. The fibers were then removed from the solution and washed with a copious amount of Nanopure water, and dried in an electrical oven at 60 °C for 6 h. The resulting fibers exhibited a porous shell on a solid graphite core.

### Fabrication of wire-like all-carbon supercapacitors

To prepare the H<sub>2</sub>SO<sub>4</sub>/PVA gel electrolyte, 6 g of H<sub>2</sub>SO<sub>4</sub> was added into 60 mL of Nanopure water, into which was added 6 g of PVA powders. The mixture was heated to 85 °C under stirring until the solution became clear. A hank of porous core-shell carbon fibers was immersed into the H<sub>2</sub>SO<sub>4</sub>/PVA solution for 5 min, keeping the pristine carbon fiber part above the solution, and then removed from the solution. After the gel was solidified at room temperature, the end of the carbon fibers that was not dipped in the H<sub>2</sub>SO<sub>4</sub>/PVA solution was split into two hanks and used as two symmetrical electrodes. After drying at ambient temperature for 12 h, a wire-like all-carbon symmetrical supercapacitor was prepared. The weight of the supercapacitor was about 200 mg, including the weights of the solid-state electrolyte/separators (H<sub>2</sub>SO<sub>4</sub>/PVA), active electrode materials (porous core-shell carbon fibers) and carbon fibers.

### Structural characterization

The surface morphologies of the samples were studied with a NOVA NANOSEM 430 field-emission scanning electron microscope (FESEM). High-resolution transmission electron

microscopic (HRTEM) images were acquired with a JEOL JEM-2100 instrument working at an acceleration voltage of 200 kV. Raman spectra were recorded using a RENISHAW inVia instrument with an Ar laser source of 488 nm in a macroscopic configuration. FTIR spectra were acquired with a NICOLET6700 spectrometer (Thermo Scientific, USA). The specific surface area and pore size distribution of the porous core-shell carbon fibers were measured using a Micromeritics ASAP 2010 with nitrogen as the adsorbate at 77 K. The desorption of nitrogen was carried out at 573 K.

### Electrochemical measurements

Cyclic voltammetric (CV) and galvanostatic charging–discharging measurements were performed in a conventional three-electrode cell with an aqueous solution of 1 M H<sub>2</sub>SO<sub>4</sub> as the electrolyte by using a CHI660E Electrochemical Workstation (CH Instruments, China). Porous core-shell carbon fibers (about 60 mg), a saturated calomel electrode (SCE, Hg/Hg<sub>2</sub>Cl<sub>2</sub>, saturated KCl) and a Pt wire were used as the working, reference and counter electrodes, respectively. The evaluation of the performance of the wire-like all-carbon supercapacitors was carried out in a two-electrode configuration using the same electrochemical workstation.

## Results and discussion

From panel (a) of Fig. 1, it can be seen that the original carbon fibers bundled rather tightly together (the upper end of the fiber in Fig. 1a), and they became apparently loosened after acid oxidation treatment, as manifested in the bottom part of panel (a). This is more clearly illustrated in the SEM measurement which clearly showed that the original carbon fibers were straight and rigid (panel b), and became curvy and flexible after acid oxidation (panel c). Interestingly, high-resolution imaging

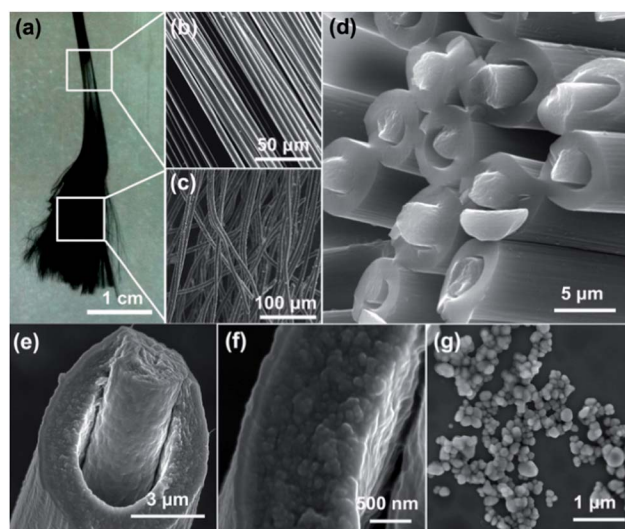


Fig. 1 (a) Photograph and (b) to (e) SEM images of porous core-shell carbon fibers, (f) carbon shell and (g) carbon particles obtained from the carbon shell by an ultrasonic treatment.

showed that the resulting carbon fibers exhibited a novel core-shell structure, as depicted in panels (d) and (e), with a core diameter of approximately 2.5  $\mu\text{m}$  and a shell thickness of about 1.5  $\mu\text{m}$ . From panels (f) and (g) it can be seen that the shell was actually composed of carbon nanoparticles of *ca.* 60 nm in diameter (Fig. S1<sup>†</sup>), presumably leading to the generation of a high surface area.

The microstructures of the carbon shells were then examined by TEM measurements. Fig. 2a depicts a porous structure of the carbon shell. A magnified TEM image from the selected area of Fig. 2a indicates that the shell is mainly composed of graphene-like carbon nanosheets (Fig. 2b), which exhibit a disordered wormhole-like porous structure at higher resolution (Fig. 2c). Moreover, these porous graphene-like nanosheets are stacked and folded together forming a hierarchical porous structure with the pore diameter largely of 3 nm and a specific pore volume of *ca.* 18  $\text{cm}^3 \text{g}^{-1}$  (Fig. S2<sup>†</sup>), which might be optimal for ion transport during the charging–discharging process.<sup>18</sup> The specific surface area was measured by the nitrogen adsorption–desorption technique at 1.087  $\text{m}^2 \text{g}^{-1}$ , markedly larger than that of the original carbon fibers (too small to be detected by the instrument). This was possibly due to the porous carbon shell with small pore diameters and solid graphite cores. In addition, the corresponding selected area electron diffraction (SAED) pattern (inset to panel b) indicates the amorphous nature of the porous carbon shell.

The structural variation was also evidenced in Raman spectroscopic measurements. From panel (e), one can see that two feature peaks emerged at 1369.6  $\text{cm}^{-1}$  (D band) and 1597  $\text{cm}^{-1}$  (G band) for the original carbon fibers. As is well-known, the D band is assigned to the vibration of carbon atoms with dangling

bonds at planar terminals of disordered graphite.<sup>19</sup> The results indicate that the carbon fibers were composed of disordered graphite domains with a large fraction of edge defects. After acid oxidation, the 2D band centered at 2720  $\text{cm}^{-1}$  was significantly intensified, suggesting enhanced structural defects within the graphene matrix.<sup>20</sup> In addition, the G band exhibited a small blue shift to 1610  $\text{cm}^{-1}$ , indicating a decrease of the number of graphene layers.<sup>21</sup> These results were consistent with the loosening of the carbon fibers and the formation of a porous core–shell structure, as highlighted in SEM and TEM measurements (Fig. 1 and 2). The structural variations before and after the acid oxidation treatment were also examined by FTIR spectroscopic measurements. As shown in Fig. S3,<sup>†</sup> no obvious vibrational bands were observed with the original carbon fibers.<sup>22</sup> After acid oxidation, several new vibrational features started to emerge: O–H stretch at 3654  $\text{cm}^{-1}$ , C=O stretch at 1798  $\text{cm}^{-1}$ , C=C stretches at 1652  $\text{cm}^{-1}$  and 1463  $\text{cm}^{-1}$ , and C–O stretch at 1068  $\text{cm}^{-1}$ , which all attest to the presence of many oxygen-containing functional groups on the porous core–shell carbon fiber surface.<sup>23</sup>

To evaluate the electrochemical performance of the porous core–shell carbon fibers, cyclic voltammetric (CV) and galvanostatic charging–discharging measurements were carried out in a three-electrode configuration in an aqueous solution of 1 M  $\text{H}_2\text{SO}_4$ , and the results are depicted in Fig. 3. From Fig. 3a, the specific capacitance of the porous core–shell carbon fibers was estimated to be 146  $\text{F g}^{-1}$  at a scan rate of 10  $\text{mV s}^{-1}$ , which was more than 410 times higher than that of the original carbon fibers (0.356  $\text{F g}^{-1}$ ). The superior performance of the core–shell carbon fibers can be ascribed to their porous structure (Fig. 1 and 2), which are beneficial for electrolyte penetration, and hence facilitates ion diffusion within the electrode materials. When the scan rate increases from 3 to 50  $\text{mV s}^{-1}$ , the specific capacitance of the porous core–shell carbon fibers decreases from 192 to 38 (Fig. S4a<sup>†</sup>), and the shape deviates from that of an ideal capacitor. This may be ascribed to the oxygenated species on the carbon electrode surface that generally exhibits relatively slow electron-transfer kinetics (this also suggests partial contributions from these faradaic processes to the electrochemical capacitance).<sup>24</sup> This may also account for the somewhat asymmetrical charging and discharging profiles (Fig. 3b) and the decrease of the specific capacitance from about 110  $\text{F g}^{-1}$  at a current density of 0.2  $\text{A g}^{-1}$  to 55  $\text{F g}^{-1}$  at 2.0  $\text{A g}^{-1}$  (Fig. S4b<sup>†</sup>). Nonetheless, it can be seen from Fig. 3c that at a current density of 0.5  $\text{A g}^{-1}$  the capacitance exhibited a negligible change from 98.0 to 96.5  $\text{F g}^{-1}$  ( $\sim 98.5\%$  retention of the capacitance) over 5000 charging–discharging cycles, indicating a very stable and recyclable electrode performance. This is likely due to the unique binder-free porous core–shell structure of the carbon fiber electrode, which allows ready and extensive uptake of ions, facilitates fast intercalation/de-intercalation of active species, and provides effective pathways for charge transport.

To test their feasibility for flexible capacitor applications, a simple wire-like all-carbon supercapacitor based on the porous core–shell carbon fibers produced above was fabricated as a demonstration. Fig. 4a shows the schematic diagram of a wire-like all-carbon supercapacitor. The electrochemical

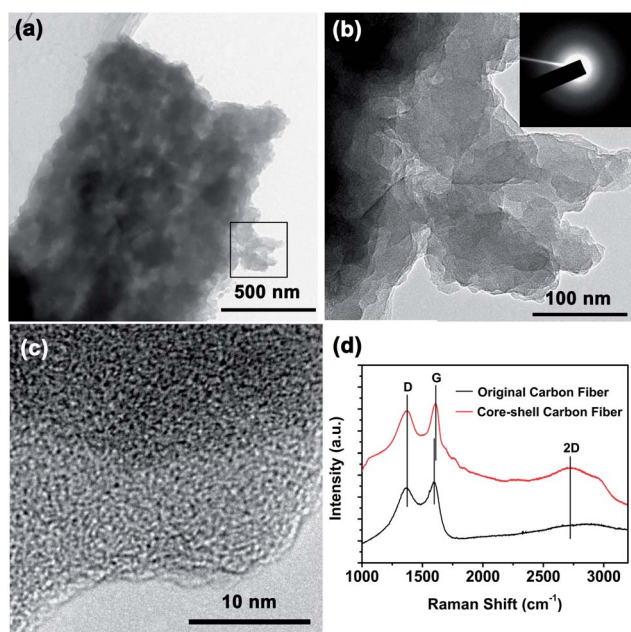


Fig. 2 (a–c) TEM images and (d) Raman spectrum of the porous core–shell carbon fibers (the spectrum of the original carbon fibers is also included). The inset to panel (b) is the SAED pattern of the porous shell of the carbon fibers.

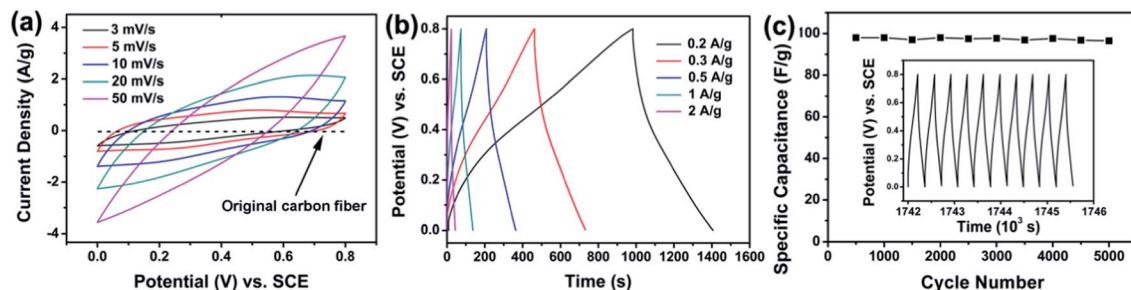


Fig. 3 (a) CV curves of a porous core-shell carbon fiber electrode at varied potential scan rates in 1 M  $\text{H}_2\text{SO}_4$  aqueous solution. The CV profile for the original carbon fiber at 10  $\text{mV s}^{-1}$  is also included as the dashed curve. (b) Galvanostatic charging-discharging curves of porous core-shell carbon fibers collected as a function of current density. (c) Cycling stability of porous core-shell carbon fibers at a current density of 1  $\text{A g}^{-1}$ . Inset: the last 10 charge-discharge curves of porous core-shell carbon fibers.

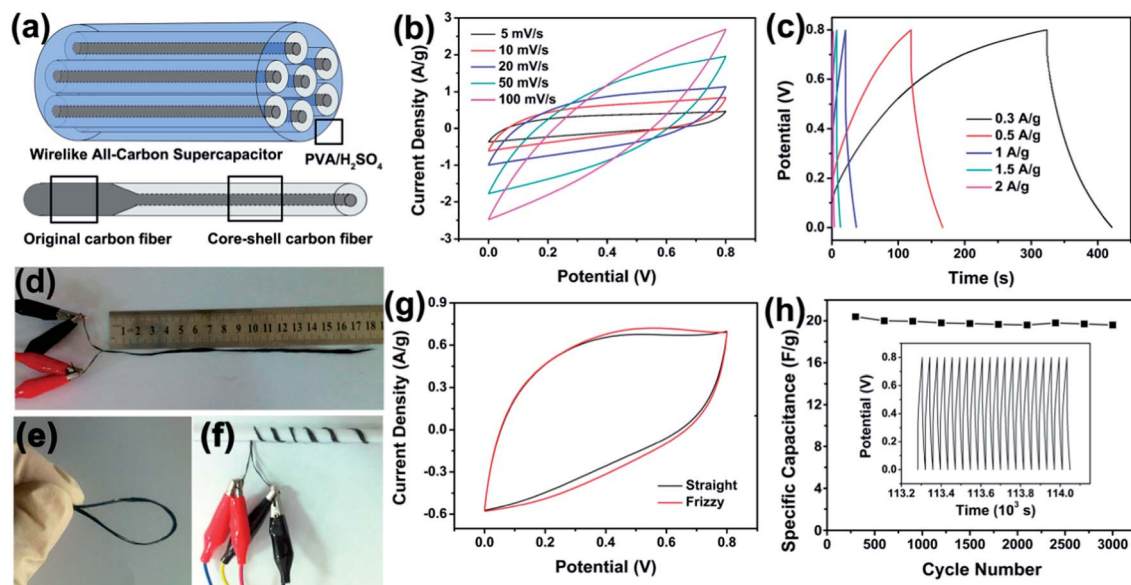


Fig. 4 (a) The schematic diagram of a fabricated wire-like all-carbon supercapacitor. (b) CV curves as a function of scan rate and (c) galvanostatic charge-discharge curves as a function of current density for a solid-state device. Photographs of (d) straight and (e and f) frizzy wire-like all-carbon supercapacitors. (g) CV curves at a scan rate of 10  $\text{mV s}^{-1}$  for the wire-like all-carbon supercapacitor in different shapes. (h) Cycle performance of wire-like all-carbon supercapacitors at 1  $\text{A g}^{-1}$  over 3000 cycles. Inset: the last 20 charge-discharge curves.

performance was analyzed using a two-electrode symmetrical supercapacitor cell in a  $\text{H}_2\text{SO}_4/\text{PVA}$  solid electrolyte. The CV curves at various potential scan rates ranging from 5 to 100  $\text{mV s}^{-1}$  and galvanostatic charging-discharging curves as a function of current density ranging from 0.3 to 2  $\text{A g}^{-1}$  are shown in Fig. 4b and c, respectively. The capacitance values calculated from the CV curve at 5  $\text{mV s}^{-1}$  and galvanostatic charging-discharging measurements at 0.3  $\text{A g}^{-1}$  are 80  $\text{F g}^{-1}$  and 37.6  $\text{F g}^{-1}$ , respectively. It is worth noting that these capacitance values were normalized to the total weight of the fiber electrode (not just the porous shell) and thus may be underestimated. The capacitances decreased from 80 to 15  $\text{F g}^{-1}$  when the scan rate increased by 20 fold from 5 to 100  $\text{mV s}^{-1}$  and from 37.6 to 4.4  $\text{F g}^{-1}$  when the current density increased by 6.7 fold from 0.3 to 2  $\text{A g}^{-1}$  (Fig. S5†). The capacitance values are somewhat smaller than those measured with a liquid electrolyte (Fig. 3), which is likely due to the increasing impedance of ion diffusion in the

solid  $\text{H}_2\text{SO}_4/\text{PVA}$  electrolyte (Fig. S6†). The wire-like all-carbon supercapacitor showed a high flexibility and can even endure twisting without apparent destruction. For instance, it can even be curled up into a ring (Fig. 4e) or spring (Fig. 4f), with no significant change of the electrochemical performance, as manifested in CV measurements (Fig. 4g). Furthermore, the supercapacitor showed long-term stability after 3000 charging-discharging cycles at 1  $\text{A g}^{-1}$ , which retained about 96% with a small decrease from 20.4 to 19.6  $\text{F g}^{-1}$  (Fig. 4h). Note that the length capacitance of the wire-like all-carbon supercapacitors (Fig. S7†) was also calculated from the CV curves at a scan rate of 10  $\text{mV s}^{-1}$  (64.5  $\text{mF cm}^{-1}$  with a length of 5 cm) and galvanostatic charge-discharge curves at a constant current of 5 mA (23.7  $\text{mF cm}^{-1}$  with a length of 5 cm). These results are better than those reported previously, such as all-solid-state supercapacitors based on graphene co-doped with nitrogen and boron (62  $\text{F g}^{-1}$  at a potential scan rate of 5  $\text{mV s}^{-1}$  in  $\text{H}_2\text{SO}_4$ /

PVA),<sup>8</sup> and nanocomposites based on carbon microfiber bundles@multiwalled carbon nanotubes (6.3 mF cm<sup>-1</sup> at a potential scan rate of 2 mV s<sup>-1</sup>, H<sub>3</sub>PO<sub>4</sub>/PVA).<sup>16</sup>

From the Ragone plot (Fig. S8†) one can see that the highest energy density of the all-solid-state supercapacitor based on porous core-shell carbon fibers is around 3.3 W h kg<sup>-1</sup> (0.37 W h cm<sup>3</sup>) at a power density of 122 W kg<sup>-1</sup> (10.1 mW cm<sup>-3</sup>), which is higher than those of polyaniline network/Au/paper (about 0.01 W h cm<sup>3</sup> in H<sub>3</sub>PO<sub>4</sub>/PVA),<sup>10a</sup> graphene oxide (0.8 mW h cm<sup>3</sup> in 1.0 M tetraethylammonium tetrafluoroborate)<sup>25</sup> and elastic fiber@carbon nanotube sheets (0.515 W h kg<sup>-1</sup> at a power density of 19 W kg<sup>-1</sup> in H<sub>3</sub>PO<sub>4</sub>/PVA).<sup>26</sup>

## Conclusions

In summary, porous core-shell carbon fibers have been synthesized by a simple and cost-effective acid oxidation treatment of carbon fibers. Supercapacitors based on the resulting porous core-shell carbon fibers showed an outstanding electrochemical performance and excellent mechanical properties, with a specific capacitance of 20.4 F g<sup>-1</sup> at a current density of 1 A g<sup>-1</sup> based on the entire device (0.41 F cm<sup>-1</sup>) and good cyclic stability (about 96% retention of capacitance after 3000 charge-discharge cycles at 1 A g<sup>-1</sup>). This remarkable performance might be attributed to the large surface area within the porous carbon shells that included agglomerates of carbon nanoparticles and the high conductance of the carbon cores. The results suggest that porous core-shell carbon fibers might be used as promising electrode materials for the fabrication of high-performance supercapacitors that are cost-effective and mechanically flexible.

## Acknowledgements

This work was supported by the National Recruitment Program of Global Experts, the PhD Start-up Funds of the Natural Science Foundation of Guangdong Province (S2013040016465), Zhujiang New Stars of Science & Technology, and the Fundamental Research Funds for Central Universities, China.

## Notes and references

- (a) P. Simon and Y. Gogotsi, *Nat. Mater.*, 2008, 7, 845; (b) K. Naoi, S. Ishimoto, J. Miyamoto and W. Naoi, *Energy Environ. Sci.*, 2012, 5, 9363; W. J. Zhou, X. H. Cao, Z. Y. Zeng, W. H. Shi, Y. Y. Zhu, Q. Y. Yan, H. Liu, J. Y. Wang and H. Zhang, *Energy Environ. Sci.*, 2013, 6, 2216.
- (a) L. L. Zhang and X. S. Zhao, *Chem. Soc. Rev.*, 2009, 38, 2520; (b) J. R. Miller, R. A. Outlaw and B. C. Holloway, *Science*, 2010, 329, 1637; (c) Y. Huang, J. J. Liang and Y. S. Chen, *Small*, 2012, 8, 1805.
- (a) Q. T. Qu, S. B. Yang and X. L. Feng, *Adv. Mater.*, 2011, 23, 5574; (b) H. L. Wang, H. S. Casalongue, Y. Y. Liang and H. J. Dai, *J. Am. Chem. Soc.*, 2010, 132, 7472.
- (a) Z. S. Wu, Y. Sun, Y. Z. Tan, S. B. Yang, X. L. Feng and K. Mullen, *J. Am. Chem. Soc.*, 2012, 134, 19532; (b) Z. J. Fan, Y. Liu, J. Yan, G. Q. Ning, Q. Wang, T. Wei, L. J. Zhi and F. Wei, *Adv. Energy Mater.*, 2012, 2, 419.
- (a) Z. Chen, V. Augustyn, J. Wen, Y. W. Zhang, M. Q. Shen, B. Dunn and Y. F. Lu, *Adv. Mater.*, 2011, 23, 791; (b) M. G. Hahm, A. L. M. Reddy, D. P. Cole, M. Rivera, J. A. Vento, J. Nam, H. Y. Jung, Y. L. Kim, N. T. Narayanan, D. P. Hashim, C. Galande, Y. J. Jung, M. Bundy, S. Karna, P. M. Ajayan and R. Vajtai, *Nano Lett.*, 2012, 12, 5616.
- (a) Z. P. Chen, W. C. Ren, L. B. Gao, B. L. Liu, S. F. Pei and H. M. Cheng, *Nat. Mater.*, 2011, 10, 424; (b) X. H. Cao, Y. M. Shi, W. H. Shi, G. Lu, X. Huang, Q. Y. Yan, Q. C. Zhang and H. Zhang, *Small*, 2011, 7, 3163.
- (a) H. Jiang, P. S. Lee and C. Z. Li, *Energy Environ. Sci.*, 2013, 6, 41; (b) Y. X. Xu, K. X. Sheng, C. Li and G. Q. Shi, *ACS Nano*, 2010, 4, 4324.
- Z. S. Wu, A. Winter, L. Chen, Y. Sun, A. Turchanin, X. L. Feng and K. Mullen, *Adv. Mater.*, 2012, 24, 5130.
- X. W. Yang, C. Cheng, Y. F. Wang, L. Qiu and D. Li, *Science*, 2013, 341, 534.
- (a) L. Y. Yuan, X. Xiao, T. P. Ding, J. W. Zhong, X. H. Zhang, Y. Shen, B. Hu, Y. H. Huang, J. Zhou and Z. L. Wang, *Angew. Chem., Int. Ed.*, 2012, 51, 4934; (b) Y. J. Kang, S. J. Chun, S. S. Lee, B. Y. Kim, J. H. Kim, H. Chung, S. Y. Lee and W. Kim, *ACS Nano*, 2012, 6, 6400; (c) L. Y. Yuan, X. H. Lu, X. Xiao, T. Zhai, J. J. Dai, F. C. Zhang, B. Hu, X. Wang, L. Gong, J. Chen, C. G. Hu, Y. X. Tong, J. Zhou and Z. L. Wang, *ACS Nano*, 2012, 6, 656.
- (a) X. H. Lu, T. Zhai, X. H. Zhang, Y. Q. Shen, L. Y. Yuan, B. Hu, L. Gong, J. Chen, Y. H. Gao, J. Zhou, Y. X. Tong and Z. L. Wang, *Adv. Mater.*, 2012, 24, 938; (b) L. H. Bao, J. F. Zang and X. D. Li, *Nano Lett.*, 2011, 11, 1215; (c) L. Yang, S. Cheng, Y. Ding, X. B. Zhu, Z. L. Wang and M. L. Liu, *Nano Lett.*, 2012, 12, 321.
- L. Zhang, F. Zhang, X. Yang, G. K. Long, Y. P. Wu, T. F. Zhang, K. Leng, Y. Huang, Y. F. Ma, A. Yu and Y. S. Chen, *Sci. Rep.*, 2013, 3, 1408.
- Y. P. Fu, X. Cai, H. W. Wu, Z. B. Lv, S. C. Hou, M. Peng, X. Yu and D. C. Zou, *Adv. Mater.*, 2012, 24, 5713.
- N. S. Liu, W. Z. Ma, J. Y. Tao, X. H. Zhang, J. Su, L. Y. Li, C. X. Yang, Y. H. Gao, D. Goldberg and Y. Bando, *Adv. Mater.*, 2013, 25, 4925.
- H. P. Cong, X. C. Ren, P. Wang and S. H. Yu, *Sci. Rep.*, 2012, 2, 613.
- V. T. Le, H. Kim, A. Ghosh, J. Kim, J. Chang, Q. A. Vu, D. T. Pham, J. H. Lee, S. W. Kim and Y. H. Lee, *ACS Nano*, 2013, 7, 5940.
- (a) J. Peng, W. Gao, B. K. Gupta, Z. Liu, R. Romero-Aburto, L. H. Ge, L. Song, L. B. Alemany, X. B. Zhan, G. H. Gao, S. A. Vithayathil, B. A. Kaiparettu, A. A. Marti, T. Hayashi, J. J. Zhu and P. M. Ajayan, *Nano Lett.*, 2012, 12, 844; (b) G. Q. He, Y. Song, K. Liu, A. Walter, S. Chen and S. W. Chen, *ACS Catal.*, 2013, 3, 831.
- J. S. Huang, B. G. Sumpter and V. Meunier, *Chem. – Eur. J.*, 2008, 14, 6614; K. S. Xia, Q. M. Gao, J. H. Jiang and J. Hu, *Carbon*, 2008, 46, 1718.
- Y. Gogotsi, J. A. Libera, N. Kalashnikov and M. Yoshimura, *Science*, 2000, 290, 317.

- 20 (a) D. Graf, F. Molitor, K. Ensslin, C. Stampfer, A. Jungen, C. Hierold and L. Wirtz, *Nano Lett.*, 2007, **7**, 238; (b) M. H. Jin, T. H. Kim, S. C. Lim, D. L. Duong, H. J. Shin, Y. W. Jo, H. K. Jeong, J. Chang, S. S. Xie and Y. H. Lee, *Adv. Funct. Mater.*, 2011, **21**, 3496.
- 21 K. N. Kudin, B. Ozbas, H. C. Schniepp, R. K. Prud'homme, I. A. Aksay and R. Car, *Nano Lett.*, 2008, **8**, 36.
- 22 S. Radic, N. K. Geitner, R. Podila, A. Kaminen, P. Y. Chen, P. C. Ke and F. Ding, *Sci. Rep.*, 2013, **3**, 2273.
- 23 S. Thakur and N. Karak, *Carbon*, 2012, **50**, 5331; H. L. Guo, M. Peng, Z. M. Zhu and L. N. Sun, *Nanoscale*, 2013, **5**, 9040.
- 24 L. Tian, D. Ghosh, W. Chen, S. Pradhan, X. J. Chang and S. W. Chen, *Chem. Mater.*, 2009, **21**, 2803.
- 25 W. Gao, N. Singh, L. Song, Z. Liu, A. L. M. Reddy, L. J. Ci, R. Vajtai, Q. Zhang, B. Q. Wei and P. M. Ajayan, *Nat. Nanotechnol.*, 2011, **6**, 496.
- 26 Z. B. Yang, J. Deng, X. L. Chen, J. Ren and H. S. Peng, *Angew. Chem., Int. Ed.*, 2013, **52**, 1.